PRNC-84

PUERTO RICO NUCLEAR CENTER

NEUTRON DIFFRACTION PROGRAM

PROGRESS SUMMARY REPORT NO. 4

M. I. KAY, I. ALMODOVAR, J. A. GONZALO,
D. T. CROMER, K. OKADA

MAY 1965 — APRIL 1966

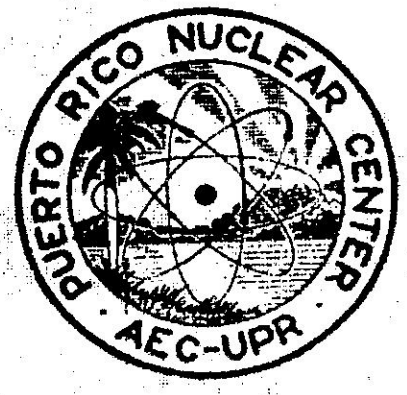

OPERATED BY UNIVERSITY OF PUERTO RICO UNDER CONTRACT
NO. AT (40-1)-1833 FOR U. S. ATOMIC ENERGY COMMISSION

PUERTO RICO NUCLEAR CENTER
NEUTRON DIFFRACTION PROGRAM

PROGRESS SUMMARY REPORT NO. 4

M.I. Kay, I. Almodovar, J.A. Gonzalo

D.T. Cromer, K. Okada

APRIL 1966

TABLE OF CONTENTS

INTRODUCTION

The neutron diffraction group at the Puerto Rico Nuclear Center has worked on essentially two types of problems. The first is concerned with the chemical binding of atoms in crystals and molecules, and the second with the nature of ferromagnetism.

Both problems are related to the spatial arrangement of atoms in molecules. If either x-rays or neutrons are scattered from crystals, patterns can sometimes be analyzed which show the arrangement of atoms in the crystal. The amplitude of x-rays diffracted from atoms is proportional to the atomic number of scattering atoms. Thus, if there are light and heavy atoms in the same compound, the contribution of the light atoms is very weak and its position can be determined only with great difficulty. If neutrons are used, however, they are scattered by the nuclei of the atoms, and as a result, diffraction of neutrons by light elements compares favorably with that from heavier elements.

There is also a neutron-electron spin interaction in compounds which possess atoms with unpaired electrons. Since the magnetic properties of substances are related to the way the electron spins are arranged within the crystal, neutron diffraction provides an accurate method for determining such spin arrangements (magnetic structures).

I. Copper Formate Tetrahydrate

Introduction

The physical properties of copper formate tetrahydrate have been extensively studied [1,2,3,4,5,6]. Phase transitions to a partially ordered magnetic state at 50°K and to an antiferromagnetic state at about 17°K have been reported. The crystal structure has been determined with x-rays by Kiriyama, Ibamoto, and Matsuo [7], who found the crystal to be monoclinic, space group $P2_1/a$ with $\underline{a}$ = 8.15, $\underline{b}$ = 8.18, and $\underline{c}$ = 6.35Å, β = 101°5' and with two formula units per unit cell. A dielectric anomaly at -38.9°C has been reported by Kiriyama [8] and independently by this laboratory [9]. In this report we give the results of a neutron diffraction analysis of the room temperature phase of copper formate tetrahydrate and an account of the dielectric anomaly.

The structure of this compound can be described as two alternating layers, one of copper formate near $\underline{z}$ = 0, see Fig. 1, and one of water near z = 1/2, see Fig. 2. It has been proposed [10] that the magnetic ordering arises from exchange through the formate groups. The Cu-Cu distance within the copper formate layers is 5.77Å. The shortest Cu-Cu distance between layers is 6.35Å, which is the $\underline{c}$ axis. A path through oxygen neighbors exists, but includes hydrogen bonds. Thus it is not surprising that a partial ordering which may be two dimentional occurs at a higher temperature than antiferromagnetism.

Preparation of Specimens

Saturated solutions of copper formate were prepared by dissolving $CuCO_3 \cdot Cu(OH)_2$ in 30% aqueous formic acid. Large single crystals were readily grown by suspending seed crystals in the solution and slowly evaporating at constant temperature (30.5°C). Crystals were cut using a wet string saw.

For dielectric measurements thin plates of dimensions 5 x 5 x 0.5 mm were cut perpendicular to the b axis. Air drying silver paint (Dupont Conductive Silver Coating Material No. 4817) was applied to serve as electrodes and then the crystal and electrodes were covered by a plastic spray to avoid dehydration.

For the neutron diffraction work parallelopipeds about 2 x 2 x 8 mm were cut along each of the three crystallographic axes. These crystals were sealed in thin glass tubes.

A drawing showing the crystal habit is given in Fig.3.

The Phase Transition

As noted in a preliminary report by Okada [9], an antiferroelectric transition occurs in copper formate tetrahydrate at -38.9°C. At this temperature the crystal shows a discontinuous decrease in dielectric constant as the temperature is lowered. A peak value of the dielectric constant 50 times as great as that observed by Kiriyama [8] was measured (Fig. 4a). Below the Curie point the crystal shows a double hysteresis loop in the curve of electric field versus polarization, within a small temperature range.

Figure 4a also shows the dielectric constant at low ac amplitude and 1000 cps versus temperature. As the temperature is decreased, the dielectric constant of the (010) plate rises to a peak of 1500 at -38.9°C and a large discontinuous decrease occurs at this temperature. Above this transition point, Tc, the Curie-Weiss law, $\varepsilon = C/(T-T_0)$, is satisfied, and a plot of the reciprocal dielectric constant versus temperature is a straight line, as seen in the figure with $T_o = -58^{\circ}C$ and $C = 3.2 \times 10^4$ °C. The (001) plate has a low dielectric constant varying gradually from 20 at room temperature to 5 at liquid-nitrogen temperature without any anomaly. The (100) plate gave a small discontinuity at T_c as shown in Fig 4a. This might be attributed to a small component of the large anomaly in the [010] direction owing to the cutting error of the crystal plate, in contrast to the perfect orientation of the (001), "as-grown" crystal plate. This high anisotropy can be expected from the predominantly layer structure of this crystal.

A clear double E-D hysteresis loop was observed within a certain temperature region below the transition point with the ordinary Sawyer-Tower hysteresis-loop circuit with a high ac amplitude of 19 kV.cm and 60 cps. At low temperature the E-D relation is a straight line. With rising temperature, nonlinearities appear at the ends of the straight line. A double hysteresis loop comes out with further warming. (see Fig. 4b).

On passing through the transition point, the loop disappears. The double hysteresis loop was observed only in a narrow temperature region from -42.6°C to the transition point. This range seemed to depend upon the applied ac amplitude.

An attempt was made to obtain saturated branches at both ends of the double loops. However, saturation in the curve of polarization versus electric field could not be obtained. When the sweeping amplitude of the AC field was not very strong, say 19 KV/cm, the double loop was quite stable. When a strong field was applied, instead of saturation, an unusual effect appeared in the critical field. The critical field decreased gradually and both loops became larger. In about one minute the loops coalesced to become a single loop similar to a distorted ferroelectric hysteresis loop. After decreasing the AC field to the field strength that had given the stable loop this procedure could be repeated. This phenomenon is similar in appearance to the AC annealing effect in a damaged ferroelectric crystal irradiated above the Curie point [10,11,12,13]. We, as yet, have no interpretation of this phenomenon and more experiments are required.

Figure 5 illustrates the thermal hysteresis in the transition. The rate of change in temperature was about 0.07°C/min. and the accuracy of temperature measurement was ± 0.05°C. The temperature was first lowered from room temperature to -63°C and then raised. A thermal hysteresis of 0.3°C occurs in the transition. Although small, this hysteresis is definitely larger than experimental error.

Effects of DC biasing fields on the transition are shown in Fig. 6. Superimposing a DC field on the 1000 cycle AC field of small amplitude used for the dielectric constant measurement moved the transition point to a lower temperature. This behavior is usual for a first order antiferroelectric phase transition.

X-ray photographs, using a precession camera and CuK_α radiation, were taken at various temperatures from room temperature, about 20°C, to -50°C. The photographs were recorded on the same film by moving the cassette a small amount for each exposure. Although no special care was taken to achieve precise measurements of the absolute lattice constants, relative values accurate to at least 0.5% were obtained. No discontinuous change, either in diffraction intensity or in lattice constants was detectable by this technique, nor did any reflections appear that violate the systematic extinctions of space group $P2_1/a$. These results are in agreement with Kiriyama [8,14] and indicate that the transition probably results from hydrogen motion. Thermal expansion coefficients are 5×10^{-5}, -2×10^{-5} and 8×10^{-5}/°C along a, b, and c respectively.

Some hk0 neutron reflections were measured below the Curie point. No reflections which should be absent in space group $P2_1/a$ were observed, but small to moderate intensity changes were noted, indicating further that the transition is caused by hydrogen motion.

Neutron Diffraction Study of the Crystal Structure

Single crystal neutron diffraction intensity measurements were made on the three principal zones of copper formate tetrahydrate at room temperature. Lorentz corrections, and in the final stages of the analysis, empirical extinction corrections were applied. Full matrix least squares refinements using isotropic temperature factors and with separate scale factors for each zone minimized $\sum w(\Delta F^2)$ where $w = 1/(\sigma F + 0.025F)$ and σF was based on counting statistics. For unobserved reflections $w = 0$.

The 00l reflections from the 0kℓ and h0ℓ zonez also had w = 0 because they were so strongly influenced by extinction. Discrepancy indices quoted are $R = \Sigma |\Delta F| / \Sigma |F_o|$ and $R_w = \Sigma w |\Delta F| / \Sigma w |F_o|$ with unobserved reflections omitted. These values are listed in Table 1.

The x-ray data of Kiriyama et al. [7] were refined by least squares using isotropic temperature factors and with weights $w = 1/(F_o + 0.02F_o^2)$. The original parameters, the least squares parameters and our final heavy atom parameters are given in Table 2.

Difference Fourier projections were computed from the neutron data with the heavy atoms removed by using the x-ray parameters of the nonhydrogen atoms found by Kiriyama et al. [7]. In these difference Fouriers we expected to find the formate hydrogen and four water hydrogens. The formate hydrogen and three of the four water hydrogens were fairly evident, but no definite indication of the fourth water hydrogen was observed.

Least squares refinement, followed by further difference Fouriers, was made with all atoms except the fourth hydrogen included. These difference Fouriers had negative regions (hydrogen has a negative scattering amplitude) near two of the symmetry centers. Neither of these positions was far enough from a center to accommodate a hydrogen atom. Placing a disordered half hydrogen in each position would result in a structure having an average of H_2O and OH^- in one position and H_2O and H_3O^+ in the other position. The latter pair is the water coordinated to the copper ion and the notion of a positive hydronium ion being coordinated to a positive copper ion is untenable. However, the existence of negative scattering regions near the symmetry centers was undeniable.

We were then lead, partly by small features in the difference Fouriers and partly by the known geometry of water, to a scheme of statistically disordered water molecules. It was this disordered water molecules. It was this disorder that led us to examine the dielectric properties of the material. This disordered structure may be regarded as a superposition of the four structures shown in Fig. 7. These are actually two similar structures and the same structures related by a center of symmetry. The hydrogen atoms H(1) and H(2) in Fig. 2 have weight 3/4 and H(3) has weight 1/2. In half of the unit cells water (1) has the orientation H(1)-OH(2), in one fourth H(1)-O-H(3) and in one fourth H(2)-O-H(3). Thus, water (1) assumes either of three positions. Water (2) also assumes either of three positions, but one bond, O-H(4), remains fixed. H(4) has unit weight, H(5) has weight 1/2 and H(6) and H(7) have weight 1/4. In half of the unit cells the orientation is H(4)-O-H(5), in one fourth it is H(4)-O-H(6) and in one fourth H(4)-O-H(7). This model was refined by least squares leading to R = 0.104 and R_w = 0.086. The resulting hydrogen parameters are given in Table 3.

From PMR measurements Kiriyama [14] assigned positions for three of the water hydrogens. She concluded that the fourth hydrogen was freely rotating about a fixed O-H(4). Her description of water (1) corresponds to our orientation H(1)-O-H(2). Her model, with the rotating water molecule, was refined by least squares resulting in R = 0.170 and R_w = 0.156. The agreement is clearly less satisfactory than for our disordered model. One might argue that the positions of H(5), H(6) and H(7) are approximations to a free rotation or minima in a hindered rotation. However, the presence of our H(3), omitted in Kiriyama's model, does seem to be necessary for good refinement of the

neutron diffraction data. The phase transition and the ease of dehydration suggest that the water molecules are not firmly bound.

Bond distances and angles are given in Table 4. Standard deviations have been calculated using the entire correlation matrix and include estimates of unit cell errors. The results for the heavy atoms are the same as obtained from the x-ray measurements within experimental error. Some of the bond lengths and angles for water appear to be in disagreement with other studies of hydrated crystals. However, the accuracy of hydrogen positions is not great. Reasons for this low accuracy are that the ratio of observations to parameters is low, high background from inelastic hydrogen scattering, and because fractional hydrogen atoms have a small scattering length, even for neutrons. Also, most of the hydrogen z parameters are near 0 or 1/2 and thus only half of the reflections, those with ℓ odd, are sensitive to the z parameters. Finally, we have postulated that the positions of all atoms are independent of the positions of all atoms are independent of the positions of the others, an assumption that is not completely correct. The higher thermal parameters for water, observed both in the x-ray and neutron studies, may indeed be a consequence of a small variation in oxygen position depending on the particular orientation of the water molecule.

There are five O-O distances of about 2.8Å. Contacts of this magnitude are generally hydrogen bonds in hydrated crystals. The proposed disorder permits all of these contacts to be hydrogen bonded all of the time. Somewhat similar disoreder is, in fact, found in ice.

this class is $NaAl(SO_4)_2 \cdot 12H_2O$. The β alum forms if the cation is large and the α alum, which is by far the most common type, occurs if the cation is of intermediate size. In all the alums there are two crystallographically different water molecules, each associated exclusively with either the monovalent or trivalent cation. The trivalent cation is always surrounded by six water molecules in a nearly regular octahedron but the orientation of the octahedron with respect to the cell axes is different in each of the three types. The monovalent cation in the α and γ alums also has six waters in a nearly regular octahedron.

The large cation in β alum can accommodate 12 oxygen neighbors. To attain this large coordination number the water octahedron is compressed along the threefold axis and stretched out normal to this axis until it is nearly planar. The two ends of the resulting trigonal antiprism are separated by only about 0.06Å. The sulfate groups at each end of this antiprism are then moved along the threefold axis toward the central cation until six sulfate oxygens are about the same distance from the cation as are the water molecules. A slightly distorted cubic close packed array of oxygens thus surround the cation.

In the γ structure six water molecules approach the small sodium cation much more closely than in the α structure. This motion cannot take place unless the hydrogen bonding system changes. The most striking result is that the sulfate groups become oppositely oriented along the threefold axis.

Discussions of the relations among the three structure have been given by Lipson [15] and by Jona and Shirane [16]. None of the alums has been investigated by modern counting techniques although Okaya, Ahmed, Pepinsky

and Vand [17] have studied monomethyl ammonium aluminum sulfate dodecahydrate (MASD) by photographic methods and refined the structure by least squares. Okaya et al. [17] do not classify MASD in a particular structure type because "the difference between α and β alum types is not adequately defined structurally". On the other hand we believe that the three structure types may be clearly distinguished and that MASD is a member of the β alums. The characteristic that distinguishes the γ alums from the α and β alums is the orientation of the sulfate group. In the γ alums this group is oriented opposite to its orientation in the α and β alums. The β alums have twelvefold and the α alums have sixfold coordination of oxygen about the central monovalent cation. Okaya et al. [17] probably overlooked this difference in coordination because the distances which they state are from the center of gravity of the $CH_3NH_3^+$ ion are actually from the nitrogen or carbon atoms of the disordered ion.

Several of the alums have been investigated using both X-ray and neutron diffraction methods. The x-ray data was taken at Los Alamos Scientific Laboratory and the Neutron Data at Puerto Rico Nuclear Center.

Cesium Alum ($Cs\ Al\ (SO_4)_2.12H_2O$)

Experimental

To grow the crystals needed for the study, fine wires were suspended in a supersaturated solution of Cs alum and numerous small crystals formed on these wires. Most of the crystals were scraped from the wires and the remainder were suspended in a saturated solution which was then allowed to evaporate slowly. An octahedron, 4 mm on an edge, was selected for study.

The crystal was briefly immersed in liquid nitrogen to increase its mosaic nature and thus reduce the effects of extinction. The neutron diffraction intensities of the hk0 zone were measured. Using a wavelength of 1.06Å, non-equivalent reflections within the range $2\theta \leq 90^{\circ}$ were measured. Of these, 64 were observed according to the criterion (I-Background) $\leq$ 2.0 X (I+Background)$^{1/2}$. Because of the large incoherent scattering,of hydrogen, absorption corrections were applied. The linear absorption coefficient for Cs alum is 4.31 cm^{-1}. Calculated transmission factors were between 0.292 and 0.353.

Refinement of the Structure with X-ray Data

The atomic positions given by Lipson [15] were used as starting values for a full matrix least squares refinement of all non-hydrogen parameters. Anisotropic thermal parameters were used in the form,

$$\exp -[B_{11}h^2 + B_{22}k^2 + B_{33}l^2 + B_{12}hk + B_{13}hl + B_{23}kl].$$

Two sets of X-ray data were taken; one with a fixed counter, fixed crystal technique, and the other using a "2θ scan" technique. The results are given in table 5. In nearly all cases the parameter differences are smaller than a standard deviation. The thermal parameters obtained from the fixed crystal data, however, are systematically slightly larger, probably because at higher angles a small portion of the intensity is lost because of $\alpha_1 - \alpha_2$ separation.

Refinement of the Structure with Neutron Diffraction Data

Structure factors were calculated by using the parameters obtained from the X-ray analysis but without any hydrogen contribution. The structure factors were initially scaled so that $\Sigma F_o = \Sigma F_c$ and a difference Fourier projection was calculated. Approximate hydrogen positions were obtained and a least squares refinement minimizing $\Sigma w(F_o - KF_c)^2$ was calculated where $w = w_E/(F_o + 0.02\ F_o^2)$. Parameters in this refinement were isotropic temperature factors for each crystallographically different atom, the scale factor and coordinates of the hydrogen atoms. The sulfur and oxygen atoms were not allowed to move. Table 6 gives the final parameter. Fig. 8 is a difference Fourier showing hydrogen atoms only.

Discussion

The interatomic distances and bond angles are given in Table 7. The errors were computed by using the entire variance-covariance matrix and include the trivial effect of lattice constant error. However, the errors in distances and angles involving hydrogen assume no error in the heavy atom positions. The anisotropic thermal parameters were transformed to obtain the thermal ellipsoid parameters which are given in Table 8.

The isotropic thermal parameters computed from the neutron data, except those for cesium and aluminum, are in good agreement with the isotropic parameters (Table 6) equivalent to the anisotropic parameters obtained from the X-ray data (18). The reason for the two exceptions is that cesium and aluminum are distinguished in projection only by their different scattering lengths

and their different thermal parameters. Therefore, the correlation between B_{Cs} and B_{Al} is large (-0.82) and is manifest in the relatively large standard deviations of these two parameters.

The octahedron about aluminum is oriented almost exactly along the cell axes and is only very slightly distorted. The Cs-$O_s(2)$ distances are a little longer than the Cs-$O_w(1)$ distances, 3.454Å vs. 3.367Å. The analogous distances in MASD are 3.42Å to $O_s(2)$ and 3.61Å to $O_w(1)$.

The sulfate group is an almost perfect tetrahedron. Rigid body analysis of the sulfate group was carried out by the method of Cruickshank [19] using a code written by Trueblood [20]. The τ and ω matrices are in Table 9. Corrections to the S-O distances were computed according to the in phase assumption of Busing and Levy [21]. The s-O distances before and after being corrected are given in Table 7. These distances agree well with other recent accurate determinations which have been tabulated by Larson (1965). The direction of maximum motion of $O_s(1)$ is normal to the S-O bond. The largest axis of the $O_s(2)$ thermal ellipsoid makes an angle of 85.7° with the S-O bond and the smallest axis makes an angle of 9.1° with the bond.

There is only one possible system of hydrogen bonding in this structure. All hydrogen atoms take part in hydrogen bonds and all oxygen atoms except $O_w(2)$ have at least one hydrogen bond. The hydrogen positions could be reasonably guessed from the heavy atoms locations obtained by x-rays. Hydrogen atoms could be clearly observed in a three dimensional difference Fourier computed with reflections having $\sin\theta/\lambda < 0.4$Å^{-1}. The O-H bond lengths were corrected for thermal motion according to Busing and Levy [21] by using the isotropic

thermal parameters obtained from the neutron diffraction data. These distances, before and after being corrected, are given in Table 7 and agree well with other neutron diffraction analysis of hydrated crystals. H(1) on $O_w(1)$ is bonded to $O_s(1)$ and this oxygen, being on a threefold axis, is bonded to three H(1) atoms. A somewhat elongated trigonal pyramid consisting of the three hydrogen atoms and the sulfur atom thus surrounds O(1). H(2) on $O_w(1)$ and H(3) on $O_w(2)$ are bonded to Os(2). These hydrogen atoms and the sulfur atom are nearly co-planar with $O_s(2)$. H(4) on $O_w(2)$ is bonded to $O_w(1)$. The angles involving H(1), H(2) and H(4) about $O_w(1)$ are nearly tetrahedral.

Hamilton [21] has given an empirical relation between O-O hydrogen bond lengths and O-H bond lengths or O-H---O angles. His empirical functions and the present experimental values are plotted in Fig. 9. The present O-H distances are systematically smaller than predicted but the differences are within the standard deviation of the measurement and the standard deviation of the prediction of the empirical function. There is no systematic trend in the O-H---O angles, all of which are nonlinear, but again the differences between the present experimental values and the empirical curve are not significant.

Although the present results are of considerably greater accuracy than those of Lipson [15], the maximum shift in atomic position in only 0.04Å.

Except as noted, all calculations on the alums were performed on an IBM 7094 at Los Alamos using codes written by Larson, Roof and Cromer [22].

Other Alums

Neutron diffraction (and X-ray data have been taken on sodium and deuterated ammonium alums). The data is now being analyzed. If these studies indicate, the structure of potassium alum will be examined to determine the role of hydrogen bonding in sulfate disorder which is rather pronounced in the potassium alum.

III. d-Tartaric Acid

The crystal structure of d-tartaric acid was determined some fifteen years ago by Stern and Beevers [23] by elegant deconvolution of the Patterson function. Although their results revealed an interesting net-work of O-H---O hydrogen bonds and the general shape of the molecule, no attempt was made to refine the structure enough so that the bond lengths and angles of this important oxyacid can be discussed with confidence. The present report deals with the refinement of the structure based on three-dimensional x-ray intensity data obtained by counter measurement on CCXD, a computer-controlled diffractometer (Cole, Okaya and Chambers), [24] and on two projections of neutron diffraction data.

The x-ray results were obtained by Okaya and Stemple of IBM Wastson Laboratory. The neutron results were collected at P.R.N.C. and the work reported jointly [25].

The cell edges from the newer x-ray work are $\underline{a}$ = 7.715Å, $\underline{b}$ = 6.004Å, $\underline{c}$ = 6.231 $\pm$.003Å. β = 100.1 $\pm$.1°. The space group is $P2_1$.

Starting from the atomic coordinates given by Stern and Beevers (23) the refinement of the structure was made from the x-ray data in the usual manner by using a full-matrix least-squares program on an IBM 7094. Only isotropic temperature factors were used for the hydrogen atoms. The atomic coordinates, their standard deviations and thermal parameters are shown in Table 10. As shown in Table 10, the isotropic temperature factors of two hydrogen atoms have become negative; although it is doubtful that any real significance can be attributed to such a result, one notices that these two hydrogen atoms are those bonded to the carbon atoms.

To confirm and refine the hydrogen positions, two (h0ℓ and hk0 zones of neutron diffraction data were taken. Because of an accident, the h0ℓ data had to be collected on two different crystals.

Refinement was carried out by means of least squares analysis, starting with the x-ray parameter set. The carbon and oxygen positional parameters (as given in Table 10) were held constant. Refinement was carried out on all the hydrogen parameters, the carbon and oxygen temperature parameters and three scale factors. The refinement proceeded with isotropic temperature factors, followed by six rounds of least squares with anisotropic temperature factors. The weights are $w = 1/(\sigma(F) + .025F)$ where $\sigma(F)$ is based on counting statistics. Non-observed reflections were given zero weight. The resultant parameters are given in Table 10.

Discussion

Bond distances and angles have been calculated from the x-ray atomic coordinates in Table 10 (a); they are shown in Figures 10 and 11, respectively. Around C(1) and C(2), only the average of the three angles involving the hydrogen atom is shown for each atom. The results of the hydrogen determination by neutron diffraction are given in Table 11 for comparison. The molecule consists of two -CH-OH-COOH parts, each part containing a planar carboxyl group and a tetrahedral -CH-OH - configuration. In each -hydroxcarboxyl group, the -hydroxyl oxygen stays close to the carboxyl plane; it is interesting to note that a similar situation also exists in the mesotartaric ion (26). It may be seen from the figures that although these two parts are similar in over-all shape, there exist slight differences. The carboxyl group of part I, C(1), C(2), O(2), and O(3), is less planar than that of part II and the O(1) - O(3) distance is much shorter than the corresponding O(4) - O(6) distance in part II; this is mainly due to the large C(4) - C(3) - O(4) angle. It is interesting to notice that such seemingly equivalent groups start to take slightly different configurations. It is difficult to decide whether this asymmetry of the molecule is due only to differences in the hydrogen-bond formation or is inherent in the tartrate ion itself. The question might be answered when accurate crystal structure analysis are made in various crystals with tartaric as well as mesotartaric ions. The planes of the two parts make an angle of 54.6°. In these two carboxyl groups which retain their protons, there are two distinct C-C-O angles; narrow C-C-OH of around 110° and wide

C-C = O of about 125°. This situation is found in many crystal structures of molecules with carboxyl groups; in case a carboxyl group loses its proton, the two C-C-O angles become almost equivalent and are about 118°. The change in the shape of carboxyl groups due to the state of ionization was exhibited in various acid salts of dicarboxylic acids, e.g. ammonium hydrogen D-tartrate (27), dipotassium ethylene-tetracarboxylate, potassium acid phthalate and others.

The structure consists of a complicated network of O-H--O hydrogen bonds. The scheme is essentially the same as that given by Stern and Beevers; the fifth contact given in their paper is ruled out as a hydrogen bond. Donohue[29] discussed the hydrogen-bond system in the crystal and proposed two possible schemes; the difference between these two schemes is based on the position of the proton on carboxyl I, i.e., the choice between O(2) and O(3) for the hydroxyl oxygen of this group. The difference in the two C-C-O angles given by Stern and Beevers leads to the conclusive evidence on the position of the proton without even locating its position; therefore, the hydrogen-bond system could have uniquely been assigned (Scheme A by Donohue) if enough data on the shape of carboxyl groups had been accumulated. As is evident from the figures and Table 12, the two carboxyl groups do not have identical surroundings; possible implication of the situation on the symmetry of the ion has been discussed in the previous paragraphs.

The neutron diffraction data confirm the hydrogen bonding scheme deduced from the x-ray data. As has been noted in previously determined compounds the values of the O-H and C-H bond distances (see Table 11). from neutron data

are, about .15Å longer than those determined from x-ray data. This discrepancy is due to an inadequate description of the x-ray scattering from a bound hydrogen. The bond distances derived from the neutron diffraction data are closer to accepted values. In addition, the two (H-O) hydrogen bond (see Table 12) angles which were found to be less than 160° by x-rays are shown to be closer to 170°. Although the accuracy of the determination is not really high enough to make the following statement with certainly, we note that the inverse relationship between O-H and O-O distance in hydrogen bonds seems to hold.

IV. The Magnetic Structure of ζ -Pd_3Mn_2

Introduction

At room temperature Pd_3Mn_2 has a tetragonally distorted CsCl type crystal structure, with (0,0,0) positions in the unit cell occupied by Pd atoms, and (1/2,1/2,1/2) positions occupied by Mn (4/5) and Pd (1/5) atoms. The arrangement of the Mn and Pd atoms in the body center position is random in the ζ-phase and is possibly ordered in the ν-phase. These differences give rise to different magnetic properties [30-34]. Recently, a detailed investigation of the magnetic and thermodynamic properties for both phases was carried out by H. Yamauchi [35], who suggested that these properties could be explained using one of two possible antiferromagnetic lattices. These have unit cells defined by $\underline{a}' = \sqrt{2}\underline{a}$, $\underline{c}' = \underline{c}$, and $\underline{a}' = \underline{a}$, $\underline{c}' = 2\underline{c}$, respectively; where the unprimed quantities refer to the chemical cell. The purpose of this investigation, which deals with the ζ-phase only, was to be ascertain,

by means of a powder neutron diffraction experiment, if one of these two models is indeed correct. The temperature dependence of magnetic peaks was examined as well.

The powder sample, obtained from the MRC Manufacturing Corporation, had been prepared by arc melting. After heat treatment of the sample above 500° and quenching in air to room temperature, the diffraction pattern was consistant with ζ-Pd_3Mn_2. The tetragonal lattice parameters, $\underline{a}$ = 2.87, and $\underline{c}$ = 3.61Å as reported by Yamauchi [6] were confirmed.

Neutron Diffraction Results

Powder neutron diffraction data were collected to an angle of $2\theta = 45^\circ$ ($\lambda = 1.06$Å) on the ζ-phase of Pd_3Mn_2 at room temperature. These data showed magnetic peaks that could be indexed on the basis of a cell with $\underline{a} = \sqrt{2}\underline{a}$ and $\underline{c}' = \underline{c}$. All magnetic reflections conform to the condition $h + k = 2\underline{n} + 1$. The new cell contains the disordered $Pd_{.2}Mn_{.8}$ atom at the positions, 1/2, 0, 1/2 and 0, 1/2, 1/2 hereafter referred to as the Mn site. The Pd atoms are at 0,0,0 and 1/2,1/2,0.

The diffraction intensities are satisfied if only the Mn moments are considered to be aligned antiferromagnetically with the spin vectors perpendicular to the $\underline{c}$ axis. If Mn alone contains an ordered moment, only the angle from the $\underline{c}$ axis may be determined [36]. A saturation moment of $4.1 \pm .2 \mu_B$ was assigned to the Mn on the basis of the observed intensity data and its temperature dependence. The observed and calculated intensities for both the nuclear and magnetic peaks are given in Table 12. The experimental Mn^{+2} form factor measured by Corliss and Hastings [37] was used.

Since some Pd moment has been observed in other PdMn alloys, other possible uniaxial models were investigated with the object of determing the possible limits of Pd contribution.

The symmetry of Pd site does not allow for an induced Pd moment and indeed no substantial improvement of the agreement is noted by assuming one. Nothing may be said about the Pd moment on the Mn site since the Mn and Pd moments for this site are extremely highly correlated.

The temperature dependence of magnetic intensities was examined from room temperature to the transition point using the magnetic (101) and the contiguous nuclear (101) reflection. The behavior of the magnetic moment as a function of temperature is given in Fig. 12 and compared with the Brillouin function for S = 4/2. The agreement is quite good. From this curve $\sigma_{R.T.}/\sigma_0 = .94$ was deduced and used in all calculations.

From the data, it was concluded that the magnetic intensity did not disappear completely until 380°C which is somewhat higher than the Neel point of 350° reported by Yamauchi [35]. This temperature difference is not surprising since Yamauchi reports that imperfect quenching or partial annealing may significantly alter the Neel temperature. Also noted was a decrease in c accompanied by an increase in a with increasing temperature in agreement with Raub et. al [32].

V. Magnetic Intensity Program

A Fortran computer program has been written to compute magnetic neutron intensities. The input consists of the atomic positions of the atoms, associated spin vectors, form factors, and indices of desired reflections.

The output is the magnetic structure factor squared of the specified reflections.

It has been used to calculate the magnetic intensities of Pd_3Mn_2, Cu Cr O_2 and Fe_2SiO_4.

This program is available as PRNC 78.

VI Conclusions

The knowledge gained from the previous studies will be briefly summerized.

The disordered hydrogen positions in copper formate tetrahydrate at room temperature have been found and some of the properties of the antiferroelectric transition at -40°C determined. The study raises many questions. Particularly, how is the structure related to the electrical effects? Since there is very little change in intensity and no change in space group in passing through the transition, a change from dynamic to static disorder may be postulated. We hope to initiate a study that will define the atomic shift caused by an electric field.

The structure including hydrogens of the three Alum $(A^{+}B^{+3})(SO_4)_2 \cdot 12H_2O$ types (α, β, γ) have been refined by means of both x-ray (Los Alamos Scientific Laboratory) and neutron diffraction (Puerto Rico Nuclear Center) data. The β Alum, Cs Al $(SO_4)_2 \cdot 12H_2O$ is reported here. Analysis is nearing completion on sodium and deutero-ammonium alums. When complete, the structure should show the effect of +1 cation size and hydrogen bonding on the structural details of the series of compounds such as the shape of the oxygen

octahedron around the +1 cation and the disorder of the sulfate group (found in some α Alums).

Neutron data has been combined with the x-ray data of Okaya and Stemple of IBM to give refinement of the structure of d-Tartaric Acid. The hydrogen bonding scheme has been unequivecally defined by the neutron data. In addition, it has been shown once again, that use of the free atom form factor will shift the hydrogen position determined from x-ray data into the bond. That is, closer to the atom to which it is most tightly bound.

The ζ -phase of Pd_3Mn_2 is antiferromagnetic. The magnetic cell is related to the tetragonal chemical cell by the transformation $a' = \sqrt{2}a$ and $c' = c$. The magnetic moment for Mn is $4.1 \pm .2 \mu_B$. The spins are aligned perpendicular to the $\underline{c}$ axis and the magnetization closely follows a Brillouin dependence from room to the Neel point.

References

1. S.A. Friedberg and R.B. Flippen, Proc. VII Int. Conf. Low Temp. Phys., 122 (1960).
2. J. Itoh and Y. Kamiya, J. Phys. Soc. Japan 17, Suppl. B-1, 512 (1962).
3. T. Haseda, R. Miedema, H. Kobayashi and E. Kanda, J. Phys. Soc. Japan 17, Suppl. B-1, 518 (1962).
4. R.B. Flippen and S.A. Friedberg, J. Chem. Phys. 38, 2652 (1963).
5. H. Kobiyashi and T. Haseda, J. Phys. Soc, Japan 18, 541 (1963).
6. S.C. Mathur and A. Mookerji, Bull, Am. Phys. Soc. 10, 254 (1965).
7. R. Kiriyama, H. Ibamoto and K. Matsuo, Acta Cryst. 7, 482 (1954).
8. H. Kiriyama, Bull, Chem. Soc. Japan 35, 1199 (1962).
9. K. Okada, Phys. Rev. Letters 15, 252 (1965).
10. L. Martin and H. Waterman, J. Chem. Soc., 1359 (1959).
11. A.G. Chynoweth, Phys. Rev. 113, 159 (1959).
12. K. Okada, J. Phys. Soc. Japan 16, 414 (1961).
13. J.A. Gonzalo and R.A. Arndt, J. Mol. Cryst. 1, to be published.
14. H. Kiriyama, Bull. Chem. Soc. Japan 35, 1205 (1962).
15. H. Lipson, Proc. Roy. Soc. A, 151, 347 (1935).
16. F. Jona and G. Shirane, Ferroelectric Crystals. International Series of Monographs on Solid State Physics, Vol. I., 335. Oxford Pergamon Press.
17. Y. Okaya, M.S. Ahmed, R. Pepinsky and V. Vand, Z. Krist. 109, 367, (1951).
18. W.C. Hamilton, Acta Cryst. 12,609 (1959).
19. D.W.J. Cruickshank, Acta Cryst. 9, 754 (1956).
20. K.N. Trueblodd, I.U.Cr. World List of Computer Programs. 1st. ed. Groningen. (1962).
21. W.C. Hamilton, Annual Review of Physical Chemistry, 13, 28, (1962).

22. W.R. Busing, and H.A. Levy, Acta Cryst. 17, 142 (1964).

23. F. Stern and C.A. Beevers, Acta Cryst 3, 341, (1950).

24. H.Cole, Y. Okaya and F.W. Chambers, Rev. Sci. Inst. 34, 872, (1963).

25. Y. Okaya, N.R. Stemple and M.I. Kay, The Crystal Structure of d-Tartaric Acid. Submitted to Acta Cryst.

26. J. Kroon, A.F. Peerdman and J.M. Vijvoet, Acta Cryst. 19, 293 (1965).

27. A.J. Van Bommel and J.M. Vijvoet, Acta Cryst. 11, 61, (1958).

28. Y. Okaya, Acta Cryst, 20, (to be published), (1966).

29. J. Donohue, J. Chem. 56, 502 (1952).

30. G. Grube, K. Bayer and H. Bumm, Z. Electrochem. 42, 805 (1936).

31. G. Grube and O. Winkler, Z. Electrochem. 42, 815 (1936).

32. E. Raub and W. Mahler, Z. Metallkunde 45, 430 (1954).

33. J.P. Burger, R. Wenling and J. Wucher, J. Phys. Radium 20, 427 (1959).

34. M.R. Wendling, Compt. Rendus 252, 408 3208 (1961).

35. H. Yamauchi, J. Phys. Soc. Japan, 19, 652 (1964).

36. G. Shirane, Acta Cryst. 12, 282 (1959).

37. L.M. Corliss, N. Elliot and J.M. Hastings, Phys. Rev. 104, 924 (1956).

38. J.W. Cable, E.O. Wollan, W.C. Koehler and H.R. Child, Phys. Rev., 128, 2118 (1962).

Table 1

Discrepancy Indices for Copper Formate Tetrahydrate

	Kiriyama et al. [7]	Least Squares Refinement of X-Ray Data		This Determination	
Zone	R	R	R_w	R	R_w
h k 0	0.10	0.090	0.108	0.092	0.071
h 0	0.12	0.096	0.113	0.101	0.080
0 k	0.11	0.094	0.104	0.120	0.116
All data		0.093	0.108	0.104	0.086

Table 2

Heavy Atom Parameters in Copper Formate Tetrahydrate

Least Squares

		Kiriyama et al.[7]	Refinement of X-Ray Data	This Determination
Cu	x	0	0	0
	y	0	0	0
	z	0	0	0
	B	1.35 Å^2	0.84 ± 0.09 Å^2	1.02 ± 0.14 Å^2
C	x	0.238	0.238 ± 0.002	0.237 ± 0.001
	y	0.270	0.268 ± 0.002	0.269 ± 0.001
	z	0.018	0.018 ± 0.002	0.024 ± 0.001
	B	1.35	0.67 ± 0.23	1.04 ± 0.16
$O_F(1)$	x	0.206	0.207 ± 0.001	0.205 ± 0.001
	y	-0.092	-0.090 ± 0.001	-0.092 ± 0.001
	z	-0.080	-0.081 ± 0.002	-0.080 ± 0.001
	B	1.35	1.47 ± 0.18	1.27 ± 0.16
$O_F(2)$	x	0.117	0.114 ± 0.001	0.116 ± 0.001
	y	0.210	0.212 ± 0.001	0.213 ± 0.001
	z	0.086	0.091 ± 0.002	0.088 ± 0.001
	B	1.35	1.10 ± 0.17	1.34 ± 0.17
$O_W(1)$	x	0.423	0.425 ± 0.001	0.430 ± 0.002
	y	0.399	0.400 ± 0.001	0.401 ± 0.002
	z	0.647	0.643 ± 0.002	0.641 ± 0.002
	B	1.35	1.76 ± 0.21	1.94 ± 0.20
$O_W(2)$	x	0.086	0.086 ± 0.002	0.089 ± 0.002
	y	0.349	0.353 ± 0.001	0.357 ± 0.002
	z	0.483	0.483 ± 0.002	0.482 ± 0.002
	B	1.35	2.10 ± 0.23	2.59 ± 0.22

Table 3

Hydrogen Parameters in Copper Formate Tetrahydrate

Atom	Weight	x	y	z	B
H_F	1	0.207 ± 0.003	0.692 ± 0.004	0.071 ± 0.004	4.2 ± 0.5 Å^2
H(1)	3/4	0.311 ± 0.003	0.385 ± 0.005	0.592 ± 0.005	3.3 ± 0.6
H(2)	3/4	0.481 ± 0.004	0.296 ± 0.004	0.592 ± 0.005	3.6 ± 0.6
H(3)	1/2	0.473 ± 0.009	0.462 ± 0.007	0.518 ± 0.015	3.9 ± 1.6
H(4)	1	0.084 ± 0.003	0.320 ± 0.003	0.339 ± 0.005	3.7 ± 0.5
H(5)	1/2	0.029 ± 0.009	0.475 ± 0.010	0.480 ± 0.017	4.7 ± 1.9
H(6)	1/4	0.195 ± 0.009	0.431 ± 0.014	0.585 ± 0.015	3.7 ± 1.7
H(7)	1/4	0.040 ± 0.007	0.269 ± 0.007	0.533 ± 0.009	0.9 ± 0.9

Table 4

Bond Distances and Angles in Copper Formate Tetrahydrate

Within the formate groups

C-O(1)	1.26 ± 0.01Å	O(1)-C-O(2)	122.0 ± 1.0°
C-O(2)	1.23 ± 0.01	H-C-O(1)	121.7 ± 1.8°
C-H	1.03 ± 0.03	H-C-O(2)	116.3 ± 1.9°

The distorted octahedron about copper

Cu-O_F(1)	1.99 ± 0.01Å	O_F(1)-Cu-O_F(2)	88.9 ± 0.4°
Cu-O_F(2)	2.00 ± 0.01	O_F(1)-Cu-O_W(1)	86.6 ± 0.4°
Cu-O_W(1)	2.38 ± 0.01	O_F(2)-Cu-O_W(1)	90.8 ± 0.4°

Water (1)

O-H(1)	0.97 ± 0.03Å	H(1)-O-H(2)	103 ± 3°
O-H(2)	1.02 ± 0.04	H(1)-O-H(3)	106 ± 5°
O-H(3)	1.04 ± 0.08	H(2)-O-H(3)	87 ± 4°

Water (2) (Only H(4) takes part in all angles because it has unit weight).

O-H(4)	0.95 ± 0.04Å	H(4)-O-H(5)	110 ± 6°
O-H(5)	1.08 ± 0.07	H(4)-O-H(6)	126 ± 5°
O-H(6)	1.15 ± 0.09	H(4)-O-H(7)	99 ± 4°
O-H(7)	0.91 ± 0.07		

Hydrogen Bonds

O_W(2)-O_F(2)	2.81 ± 0.02Å	O_W(2)-H(4)-O_F(2)	166 ± 3°
H(4)-O_F(2)	1.88 ± 0.03		
O_W(1)-O_W(1)	2.81 ± 0.03	O_W(1)-H(3)-O_W(1)	166 ± 7°
H(3)-O_W(1)	1.79 ± 0.07		
O_W(2)-O_W(2)	2.78 ± 0.03	O_W(2)-H(5)-O_W(2)	167 ± 9°
H(5)-O_W(2)	1.72 ± 0.07		
O_W(1)-O_W(2)	2.81 ± 0.02	O_W(1)-H(1)-O_W(2)	176 ± 3°
H(1)-O_W(2)	1.84 ± 0.03	O_W(1)-H(6)-O_W(2)	132 ± 8°
H(6)-O_W(1)	1.90 ± 0.08		
O_W(1)-O_W(2)	2.76 ± 0.02	O_W(1)-H(3)-O_W(2)	169 ± 3°
H(3)-O_W(2)	1.75 ± 0.04	O_W(1)-H(7)-O_W(2)	176 ± 6°
H(7)-O_W(1)	1.85 ± 0.07		

Oxygens related by centers of symmetry

Table 5

Least squares parameters for $CsAl(SO_4)_2 \cdot 12H_2O$ from X-ray diffraction data
The upper numbers are from the fixed crystal data and the lower numbers
from the 2θ scan data. $w = w_E/(F_o + 0.02F_o^2)$ in both cases

Atom	x	y	z	$B_{11}x10^5$	$B_{22}x10^5$	$B_{33}x10^5$	$B_{12}x10^5$	$B_{13}x10^5$	$B_{23}x10^5$
Cs	0.5	0.5	0.5	428±7	B_{11}	B_{11}	-88±10	B_{12}	B_{12}
	0.5	0.5	0.5	404±7	B_{11}	B_{11}	-84±15	B_{12}	B_{12}
Al	0.0	0.0	0.0	218±15	B_{11}	B_{11}	54±36	B_{12}	B_{12}
	0.0	0.0	0.0	186±15	B_{11}	B_{11}	18±50	B_{12}	B_{12}
S	0.32867±15	x	x	217±9	B_{11}	B_{11}	59±22	B_{12}	B_{12}
	0.32865±19	x	x	211±11	B_{11}	B_{11}	60±31	B_{12}	B_{12}
O (1)	0.25955±40	x	x	402±34	B_{11}	B_{11}	-220±66	B_{12}	B_{12}
	0.25935±48	x	x	384±38	B_{11}	B_{11}	-241±87	B_{12}	B_{12}
$O_s(2)$	0.27893±42	0.34108±42	0.43637±40	486±43	340±41	250±38	143±70	313±67	91±65
	0.27869±53	0.34096±55	0.43681±49	484±53	338±54	212±47	150±93	331±81	133±82
$O_w(1)$	-0.15928±43	0.05065±43	0.28465±40	323±40	366±40	401±39	10±70	116±69	25±70
	-0.15917±57	0.05129±54	0.28488±52	285±53	358±50	390±50	-6±89	162±90	-5±86
$O_w(2)$	0.15236±41	-0.00199±37	0.00001±40	203±34	329±38	399±42	40±69	103±63	-3±63
	0.15261±44	-0.00209±50	-0.00138±56	187±38	308±42	385±45	21±101	50±86	54±91
g	$1.74±31x10^{-7}$								
	$1.58±32x10^{-7}$								

Table 6

Least squares parameters for $CsAl(SO_4)_2 \cdot 12H_2O$ from neutron diffraction data
Equivalent isotropic thermal parameters from X-ray data are in parenthesis.

Atom	B	x	y	z
H(1)	2.8 ± 0.7	0.624 ± 2	0.219 ± 2	0.181 ± 2
H(2)	2.2 ± 0.5	0.730 ± 2	0.222 ± 2	0.993 ± 3
H(3)	1.6 ± 0.4	0.694 ± 2	0.064 ± 2	0.514 ± 2
H(4)	2.7 ± 0.6	0.532 ± 3	0.203 ± 4	0.555 ± 3
Cs	5.1 ± 3.1 (2.6)			
Al	0.5 ± 1.3 (1.3)			
S	1.5 ± 0.7 (1.3)			
$O_s(1)$	3.9 ± 0.7 (2.5)			
$O_s(2)$	2.2 ± 0.3 (2.2)			
$O_w(1)$	1.8 ± 0.3 (2.2)			
$O_w(2)$	1.9 ± 0.2 (1.9)			

Table 7

Interatomic distances and angles in $CsAl(SO_4)_2 \cdot 12H_2O$
from fixed crystal and neutron diffraction data.
Standard deviations in parentheses, apply to the right most digit
Distances corrected for thermal motion are in parentheses.

Al - 6 $O_w(1)$	1.882(5)Å		
Cs - 6 $O_w(1)$	3.367(5)		
- 6 $O_s(2)$	3.454(5)		
The sulfate group			
S - $O_s(1)$	1.479(9)	$O_s(1)$-S-$O_s(2)$	109.9(2)°
	(1.496)	$O_s(2)$-S-$O_s(2)$	109.0(2)
S - 3 $O_s(2)$	1.473(5)	$O_s(2)$-$O_s(2)$-$O_s(2)$	60.0
	(1.485)	$O_s(2)$-$O_s(2)$-$O_s(1)$	60.2(1)
$O_s(1)$-3 $O_s(2)$	2.417(8)	$O_s(2)$-$O_s(1)$-$O_s(2)$	59.5(3)
$O_s(2)$-2 $O_s(2)$	2.399(8)		
Water molecules			
$O_w(1)$-H(1)	0.941(26)	H(1)-$O_w(1)$-H(2)	107.6(24)
	(0.955)		
$O_w(1)$-H(2)	0.963(29)		
	(0.968)		
$O_w(2)$-H(3)	0.974(26)	H(3)-$O_w(1)$-H(4)	107.2(20)
	(0.974)		
$O_w(2)$-H(4)	0.984(36)		
	(0.995)		
Hydrogen bonds			
$O_s(1)$-3 $O_w(1)$	2.822(6)	$O_s(1)$-H(1)-$O_w(1)$	165(2)
$O_s(1)$-3 H(1)	1.902(25)		
$O_s(2)$- $O_w(1)$	2.766(7)	$O_s(2)$-H(2)-$O_w(1)$	171(3)
$O_s(2)$- H(2)	1.811(29)		
$O_s(2)$-$O_w(2)$	2.648(7)	$O_s(2)$-H(3)-$O_w(2)$	166(3)
$O_s(2)$-H(3)	1.692(27)		
$O_w(1)$-$O_w(2)$	2.615(7)	$O_w(1)$-H(4)-$O_w(2)$	163(3)
$O_w(1)$-H(4)	1.657(33)		
Miscellaneous angles			
Al-$O_w(2)$-H(3)	121(2)°	H(1)-$O_s(1)$-H(1)	102(1)°
Al-$O_w(2)$-H(4)	130(2)	H(1)-$O_s(1)$-S	116(1)
H(3)-$O_w(2)$-H(4)	107(2)		
H(1)-$O_w(1)$-H(4)	109(2)	H(2)-$O_s(2)$-H(3)	101(1)
H(2)-$O_w(1)$-H(4)	116(2)	S - $O_s(2)$-H(2)	119(1)
H(1)-$O_w(1)$-H(2)	108(3)	S - $O_s(2)$-H(3)	131(1)

Table 8

Thermal ellipsoids in $CsAl(SO_4)_2 \cdot 12H_2O$, fixed crystal data

Atom	RMS Amplitude	B_i	Direction angles relative to crystal axes		
					γ
Cs	0.162 ± 3 Å	2.08 ± 7 Å^2	54.7°	54.7°	54.7°
	0.191 ± 2	2.88 ± 5	-	-	-
	0.191 ± 2	2.88 ± 5	-	-	-
Al	0.145 ± 11	1.66 ± 25	54.7	54.7	54.7
	0.122 ± 7	1.17 ± 14	-	-	-
	0.122 ± 7	1.17 ± 14	-	-	-
S	0.146 ± 7	1.68 ± 15	54.7	54.7	54.7
	0.120 ± 5	1.14 ± 9	-	-	-
	0.120 ± 5	1.14 ± 9	-	-	-
$O_s(1)$	0.119 ± 22	1.11 ± 42	54.7	54.7	54.7
	0.199 ± 10	3.13 ± 32	-	-	-
	0.199 ± 10	3.13 ± 32	-	-	-
$O_s(2)$	0.214 ± 9	3.63 ± 29	33 ± 5	72 ± 7	64 ± 4
	0.155 ± 10	1.91 ± 25	108 ± 9	19 ± 7	95 ± 13
	0.118 ± 12	1.10 ± 23	116 ± 6	93 ± 13	26 ± 5
$O_w(1)$	0.150 ± 10	1.78 ± 25	28 ± 14	89 ± 28	118 ± 13
	0.168 ± 9	2.22 ± 25	96 ± 28	11 ± 28	99 ± 28
	0.183 ± 9	2.66 ± 27	63 ± 13	79 ± 27	30 ± 14
$O_w(2)$	0.120 ± 11	1.15 ± 21	16 ± 9	98 ± 14	104 ± 8
	0.160 ± 9	2.02 ± 23	83 ± 15	8 ± 14	94 ± 22
	0.178 ± 9	2.51 ± 26	76 ± 8	88 ± 22	14 ± 10

Table 9

Translation and torsional vibration matrices
for the sulfate group relative to the unit cell axes

$$T = \begin{pmatrix} 0.0160 & 0.0015 & 0.0015 \\ & 0.0160 & 0.0015 \\ & & 0.0160 \end{pmatrix} \text{Å}^2 ; \quad \omega = \begin{pmatrix} 29.2 & -8.8 & -8.8 \\ & 29.2 & -8.8 \\ & & 29.2 \end{pmatrix} \text{deg}^2$$

$$\sigma(T) = \begin{pmatrix} 0.0020 & 0.0017 & 0.0017 \\ & 0.0020 & 0.0017 \\ & & 0.0020 \end{pmatrix} \text{Å}^2 ; \quad \sigma_\omega = \begin{pmatrix} 5.1 & 3.9 & 3.9 \\ & 5.1 & 3.9 \\ & & 5.1 \end{pmatrix} \text{deg}^2$$

TABLE 10 (a). Atomic coordinates in fractions of cell edges and their standard deviations in 10^{-4}A, (the deviations for hydrogen atoms are in 10^{-3}A).

Atoms	x	(x)	y	(y)	z	(z)
O(1)	0.3382	26	0.0343	25	0.5102	21
O(2)	0.4296	27	-0.0325	27	-0.0219	23
O(3)	0.6084	24	0.0050	26	0.3005	22
O(4)	0.3063	25	0.4173	25	0.2335	22
O(5)	-0.0765	28	0.0792	32	0.1790	28
O(6)	-0.0217	27	0.4072	33	0.3496	29
C(1)	0.2941	33	0.0159	34	0.2832	30
C(2)	0.4640	34	-0.0068	35	0.1911	31
C(3)	0.2003	32	0.2273	33	0.1811	29
C(4)	0.0219	35	0.2528	35	0.2496	31
H(1)	0.241	36	-0.116	36	0.236	29
H(2)	0.182	33	0.207	35	0.028	31
H(3)	0.253	93	0.037	85	0.555	72
H(4)	0.515	81	-0.046	69	-0.090	57
H(5)	0.342	54	0.438	64	0.367	56
H(6)	-0.182	85	0.049	67	0.203	54
Neutron Diffraction Results						
H(1)	0.2101	21	-0.1385	28	0.2256	34
H(2)	0.1699	15	0.1993	45	0.0032	18
H(3)	0.2359	14	-0.0177	35	0.5724	19
H(4)	0.5360	15	-0.0427	26	-0.0931	23
H(5)	0.3470	21	0.4329	46	0.3900	22
H(6)	-0.1928	12	0.0725	27	0.2315	24

(b) Anisotropic Temperature Factors: The betas are used in the expression

$$\exp -(B_{11}h^2 + B_{22}k^2 + B_{33}l^2 + B_{12}hk + B_{13}hl + B_{23}kl)$$

	B_{11}	B_{22}	B_{33}	B_{12}	B_{13}	B_{23}
O(1)	0.006954	0.023553	0.011499	-0.000061	0.005686	0.005782
O(2)	0.007255	0.027130	0.014123	0.003722	0.008140	-0.005980
O(3)	0.005784	0.023744	0.016340	0.002330	0.006068	0.008815
O(4)	0.006482	0.017080	0.010[illegible]	-0.004009	0.003432	0.001163
O(5)	0.006407	0.026887	0.023627	-0.007638	0.010231	-0.017242
O(6)	0.009209	0.026419	0.024926	-0.000048	0.013101	-0.017736
C(1)	0.005103	0.014112	0.012669	0.002223	0.003880	0.003362
C(2)	0.006652	0.011615	0.015023	-0.000247	0.005570	0.003338
C(3)	0.004421	0.015322	0.009547	-0.000097	0.00[illegible]342	0.000672
C(4)	0.004968	0.018028	0.012031	0.001643	0.000526	-0.000434

Isotropic temperature factors for hydrogen atoms, in 10 - 16 cm^2

H(1)	H(2)	H(3)	H(4)	H(5)	H(6)
-1.3	-1.2	6.4	4.4	1.8	5.3

Table 11

(a) Bond distances involving hydrogen atoms from coordinates determined from the neutron study.

O(1) - H(3)	0.98 ± .02
O(2) - H(4)	1.00 ± .02
O(4) - H(5)	0.97 ± .02
O(5) - H(6)	1.00 ± .02
C(1) - H(1)	1.15 ± .03
C(3) - H(2)	1.14 ± .02

(b) Bond angles in degrees around oxygens

C(1) - O(1) - H(3)	108 ± 3
C(2) - O(2) - H(4)	115 ± 3
C(3) - O(4) - H(5)	112 ± 3
C(4) - O(5) - H(6)	115 ± 4

around C(1)

H(1) - C(1) - O(1)	114 ± 3
H(1) - C(1) - C(2)	107 ± 3
H(1) - C(1) - C(3)	110 ± 3

around C(3)

H(2) - C(3) - O(4)	111 ± 4
H(2) - C(3) - C(1)	107 ± 4
H(2) - C(3) - C(4)	105 ± 4

TABLE 12 Hydrogen-bond system in the D-tartaric acid crystal. The second values for H-O, H..O and angles around hydrogens are those obtained by the neutron study.

Bonds	A	B	C	D
From	O(1)	O(4)	O(2)	O(5)
To	O(6)	O(3)	O(4)	O(3)
Of	$(-x, -\frac{1}{2} + y, 1-z)$	$(1-x, \frac{1}{2} + y, 1-z)$	$(1-x, -\frac{1}{2} + y, -z)$	$(-1 + x, y, z)$
Hydrogen involved	H(3)	H(5)	H(4)	H(6)
Distances (A)	2.839	2.909	2.633	2.707
O-H	0.8, 0.98	0.8, 0.97	0.9, 1.00	0.9, 1.00
H---O	2.1, 1.86	2.1, 1.95	1.8, 1.64	1.9, 1.71
Angles around hydrogens	157°, 171°	172°, 169°	176°, 172°	152°, 168°
Separations listed by Stern and Beevers	$O_1 - O_{10}$	$O_7 - O_5$	$O_4 - O_7$	$O_5 - O_9$

TABLE 13 A comparison of the observed and calculated intensities (a) from Pd_3Mn_2 at T = 297°K.

hkl	Iobs	$(Icalc)_N$	$(Icalc)_M$	O/Iobs
M(100)	26.2		26.7	0.05
001	28.7	27.7		0.05
100	33.2	34.9		0.04
M(101)	26.0		24.3	0.05
101	14.3	13.1		0.07
110	5.6	5.4		0.15
M(210)			2.4	
002	31.4	2.1		0.09
111		27.0		
M(102)	5.5		3.1	0.15
M(211)			3.5	
102	17.7	20.6		0.07
200	2.7	2.9		0.15

(a) Both nuclear and magnetic intensities given are per chemical unit cell. $b_{Pd} = 0.59 \times 10^{-12}$ cm., $b_{Mn} = 0.36 \times 10^{-12}$ ec.; 2B = 1.0Å.

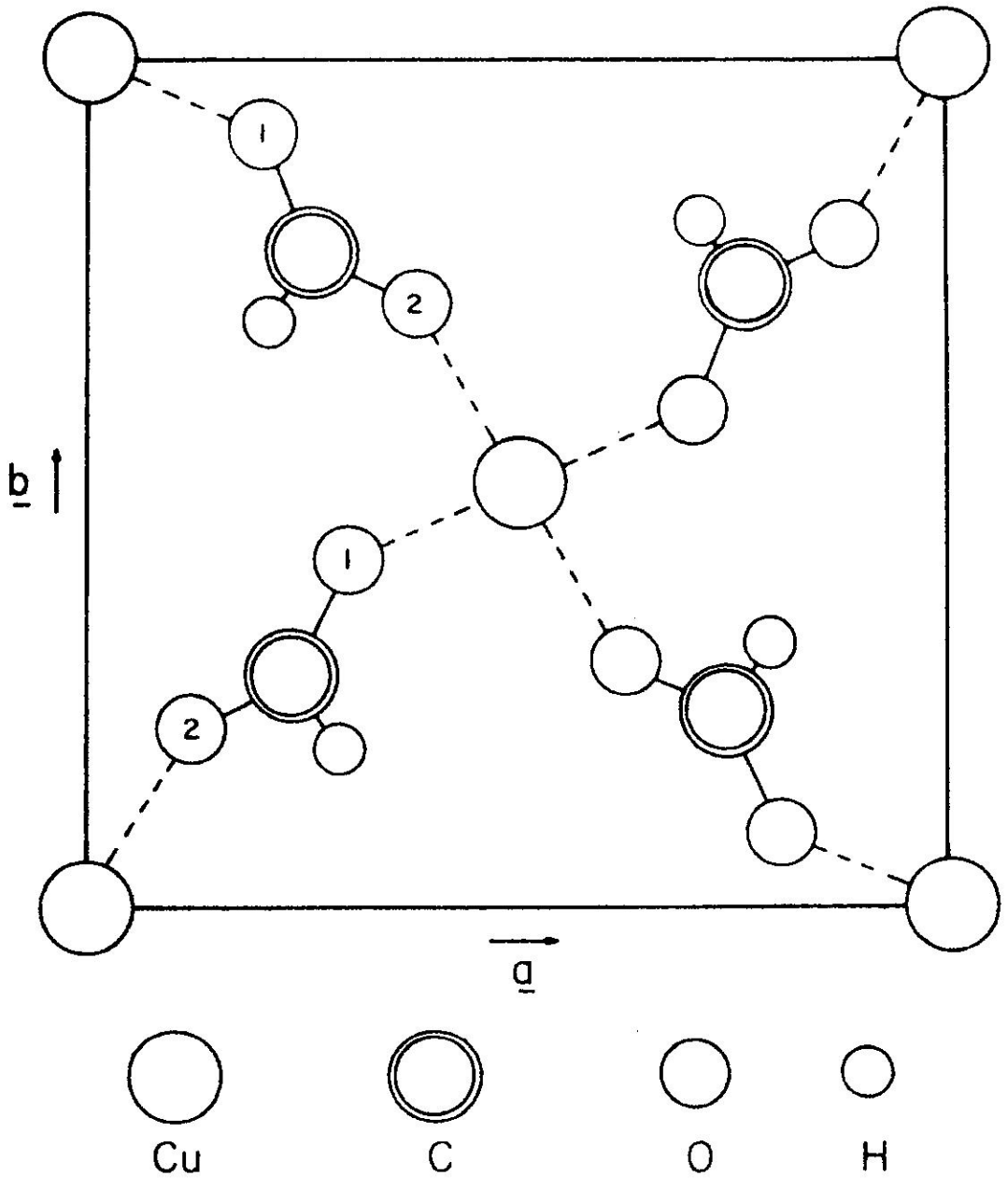

Fig. 1 Copper formate layer near $\underline{z} = 0$.

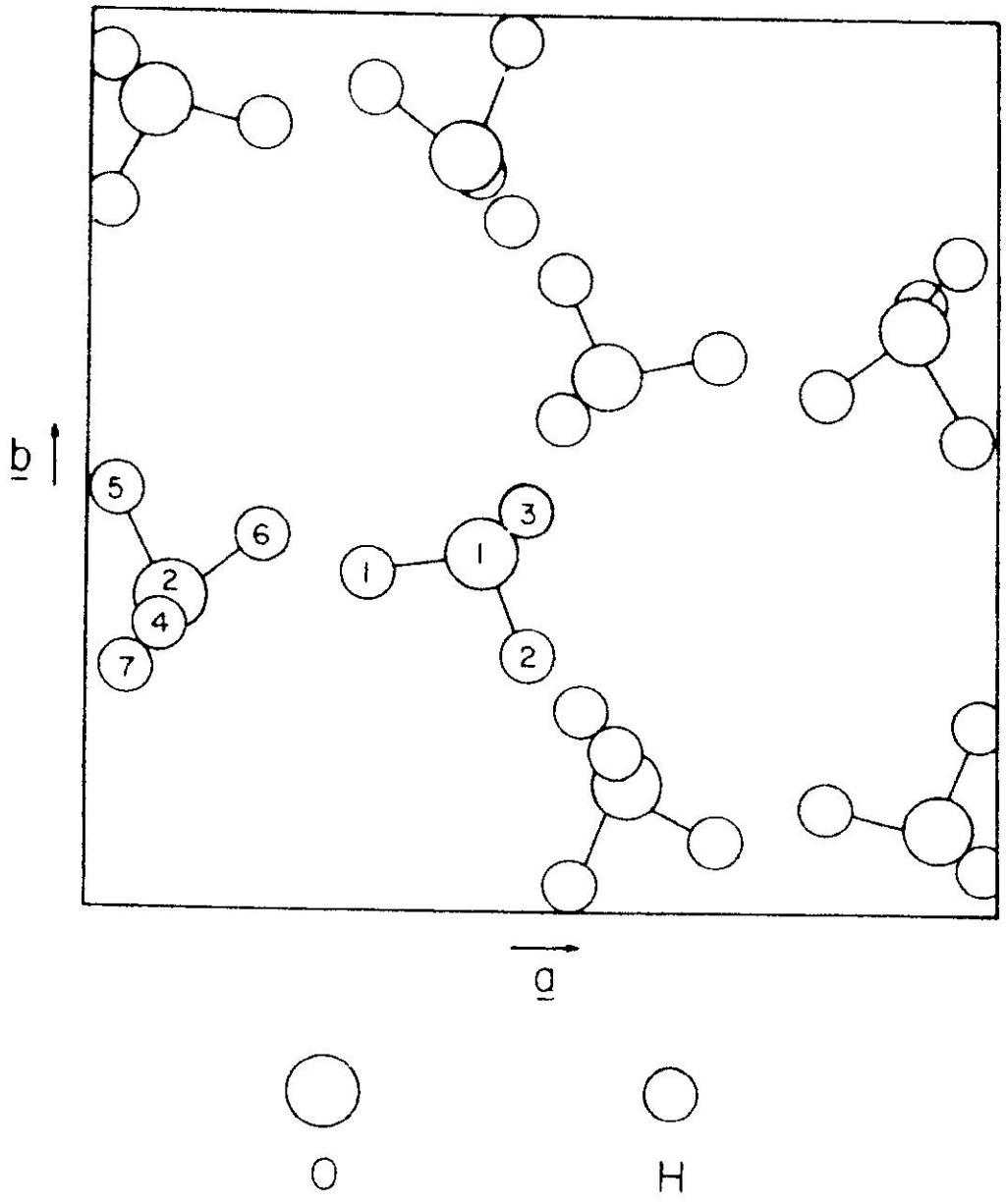

Fig. 2 Water layer near $\underline{z} = 1/2$ showing disordered hydrogen positions as explained in text.

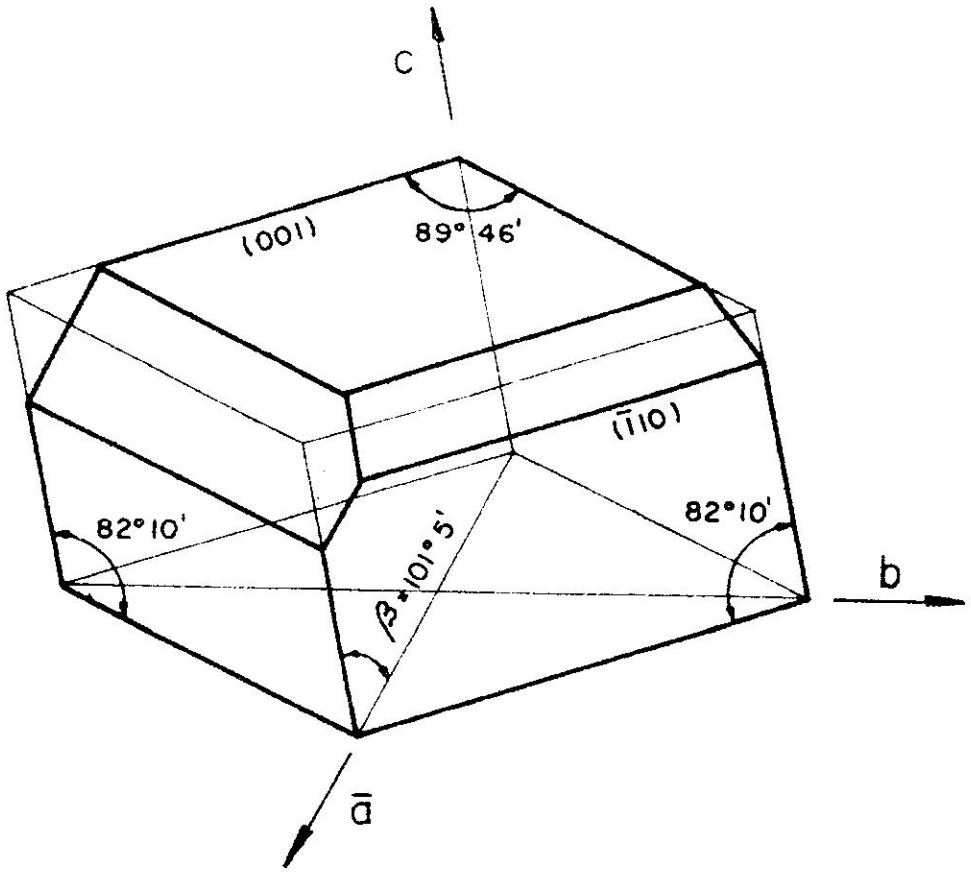

Fig. 3 Crystal habit of $Cu(HCOO)_2 \cdot 4H_2O$

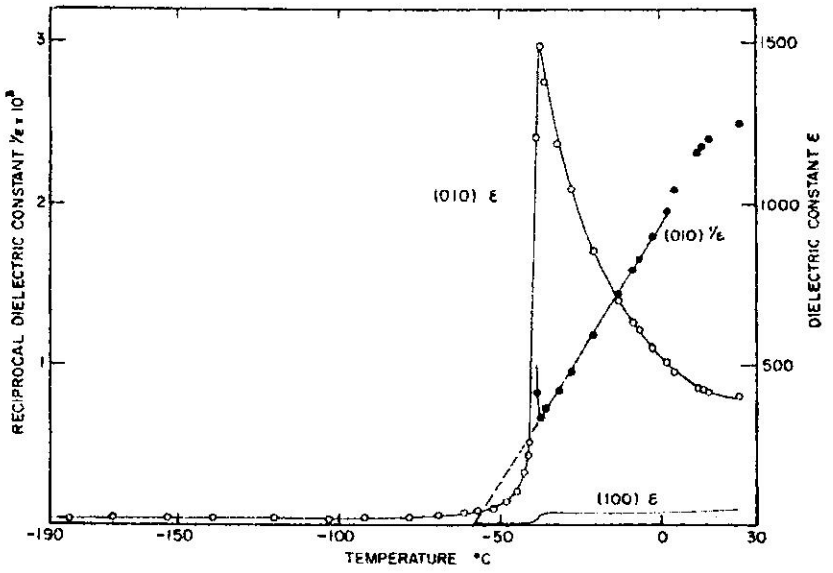

Fig. 4a Dielectric constant versus temperature in copper-formate tetrahydrate at 1000 cps.

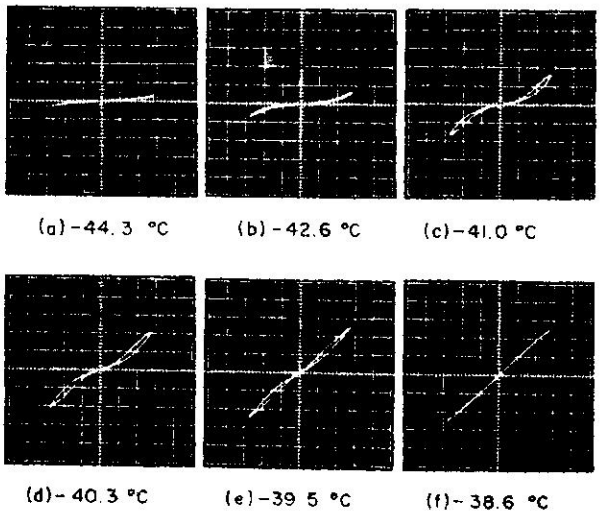

Fig. 4b Double hysteresis loops of (010) copper-formate tetrahydrate plate at various temperatures below T_c at 60 cps. Sweeping amplitude: 19 kV/cm.

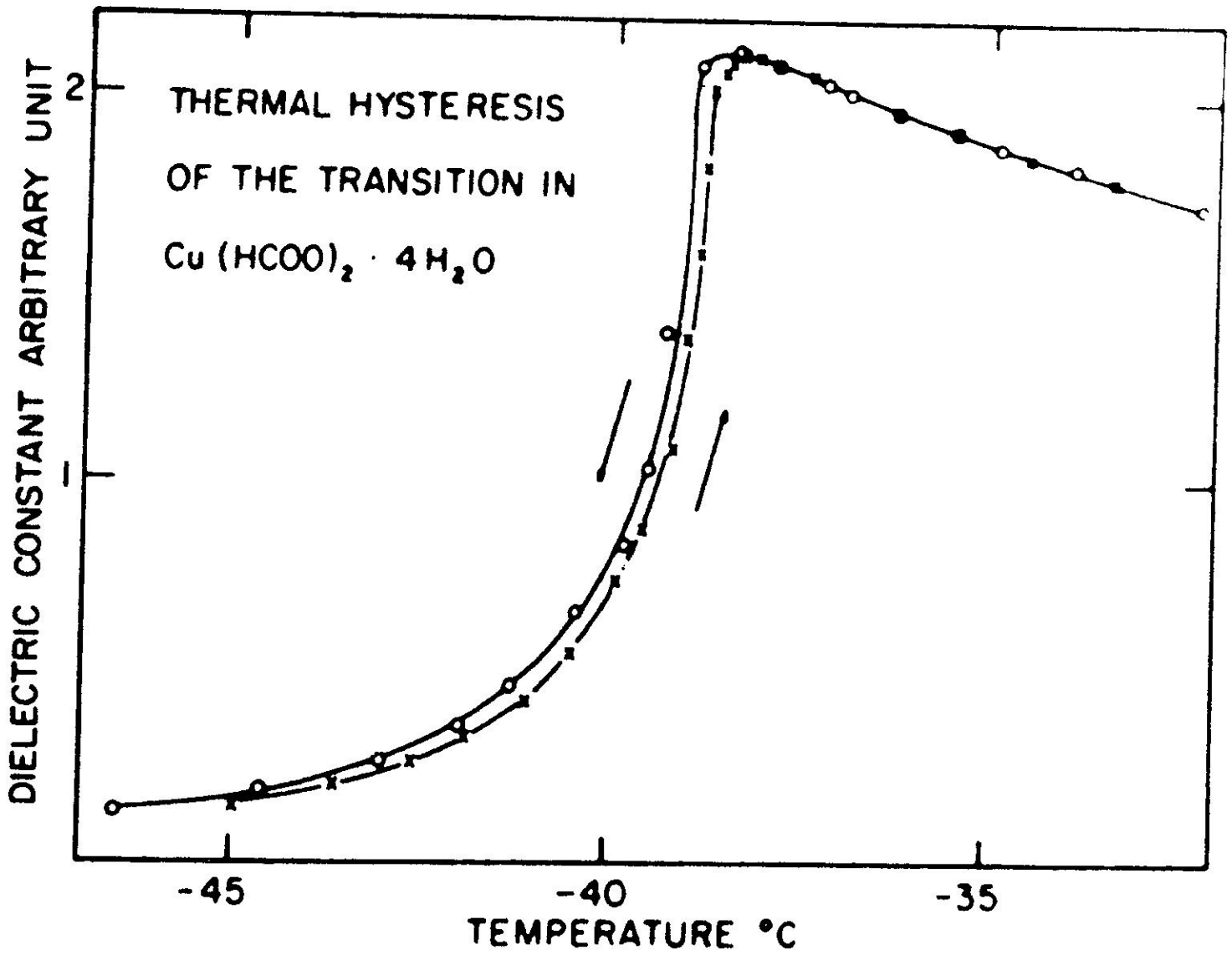

Fig. 5 Thermal hysteresis of the antiferroelectric transition in $Cu(HCOO)_2 \cdot 4H_2O$.

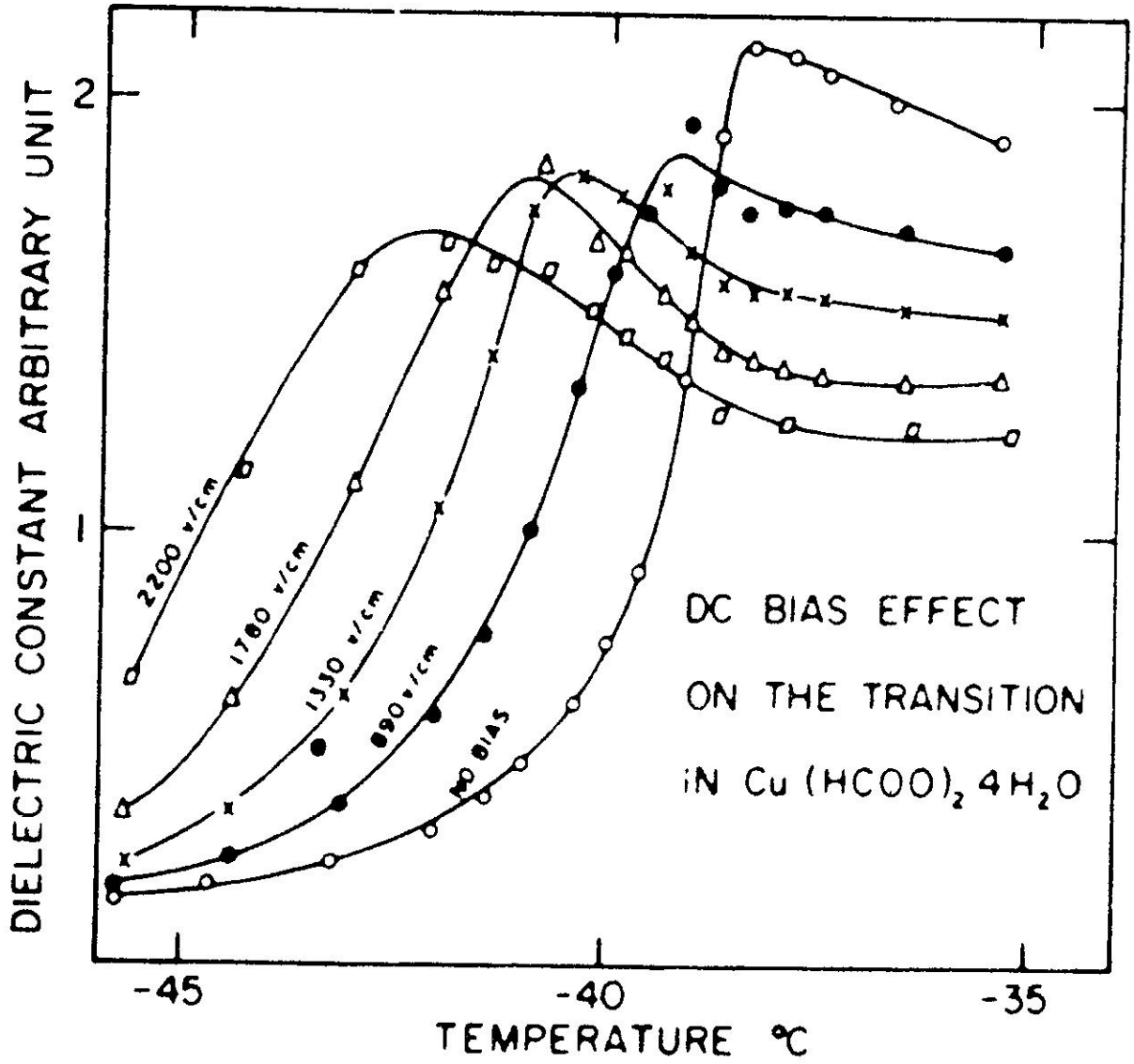

Fig. 6 The effect of DC bias on the antiferroelectric transition in $Cu(HCOO^{-})_2$

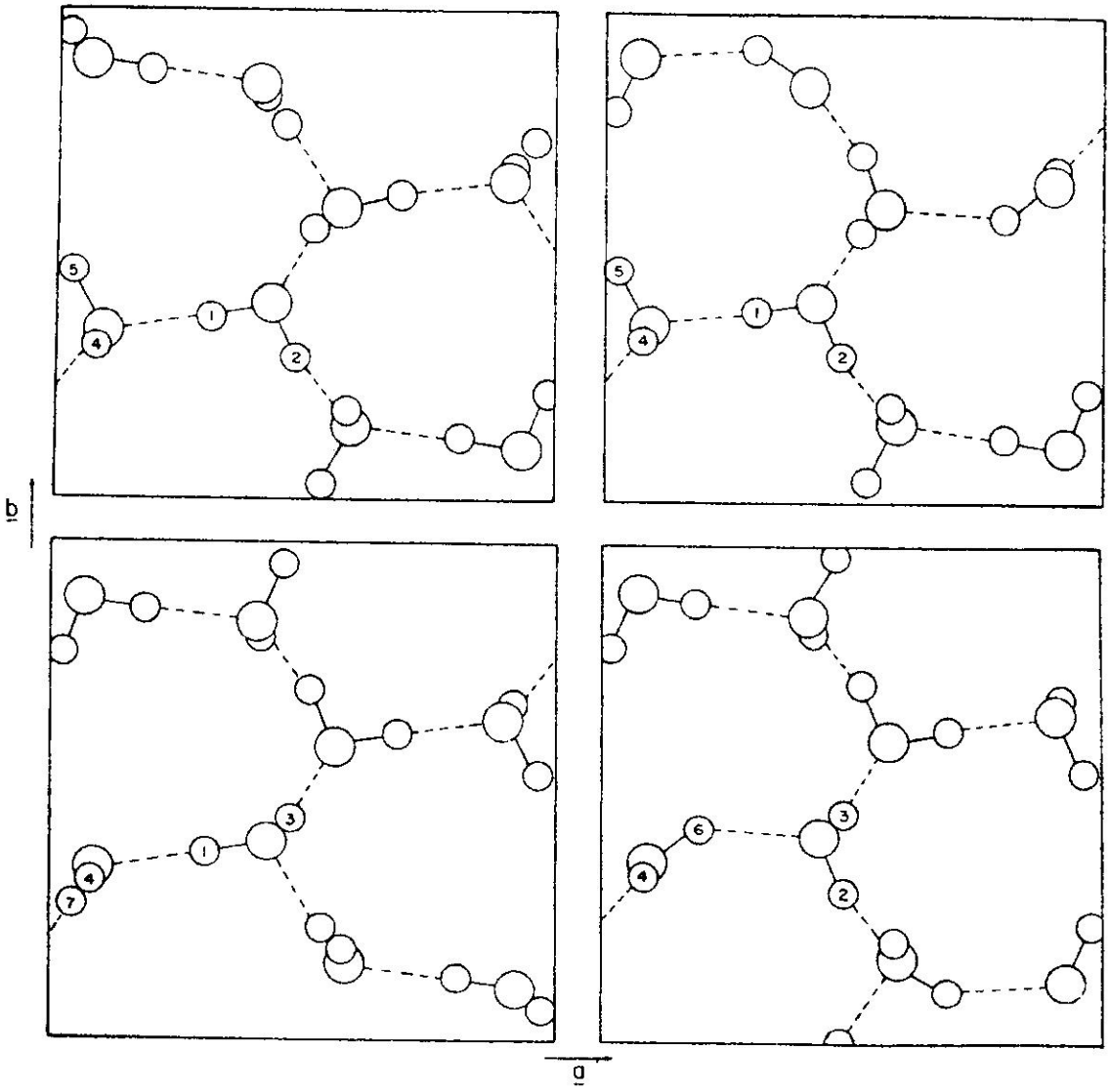

Fig. 1 Four water arrangements which when superimposed give the structure shown in Fig. 2.

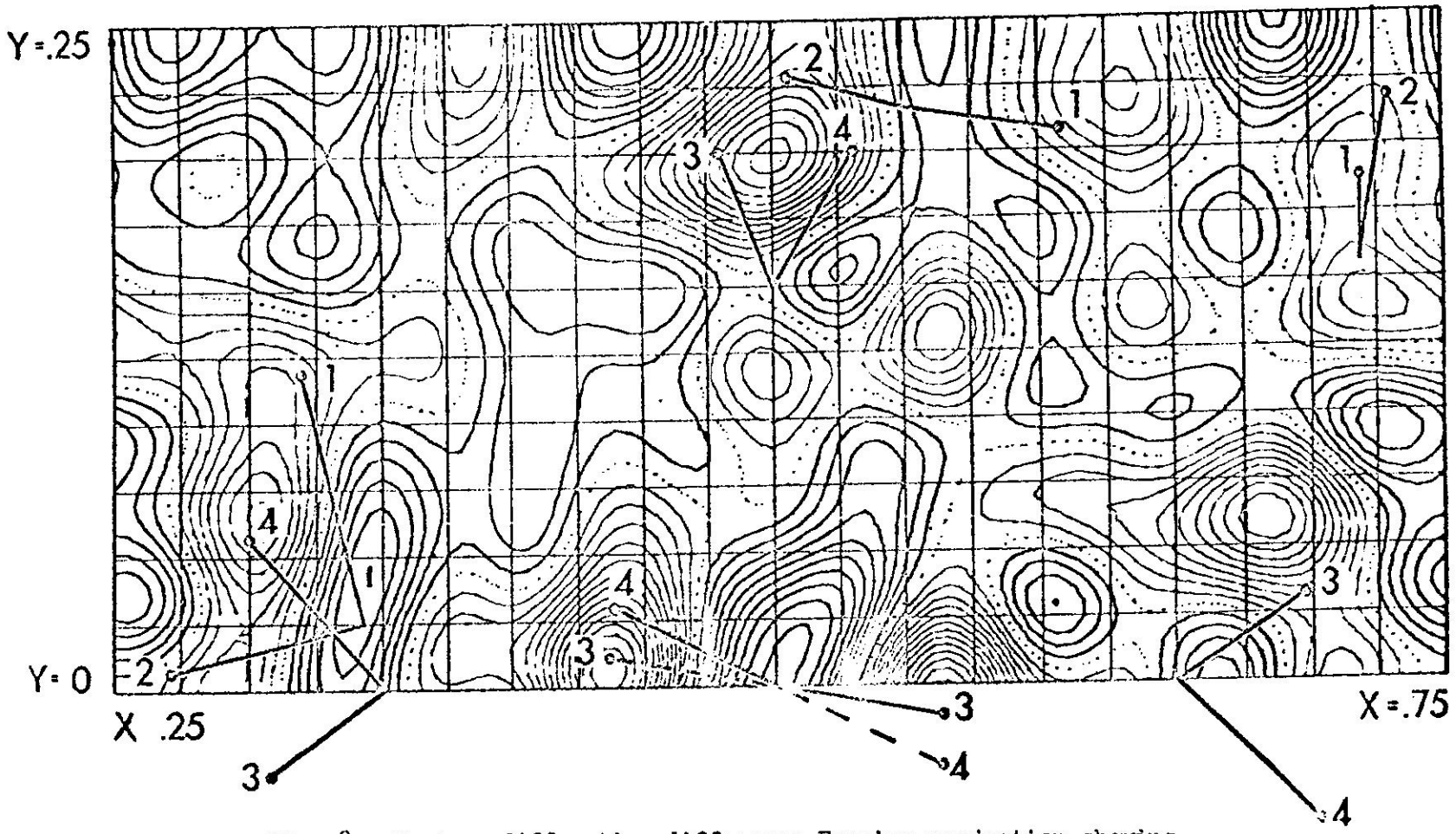

Fig. 8 Neutron diffraction difference Fourier projection showing hydrogen atoms only. Contours are at equal arbitrary units. Heavy lines are positive contours, light lines negative and the zero contour is dotted. Cs Alum

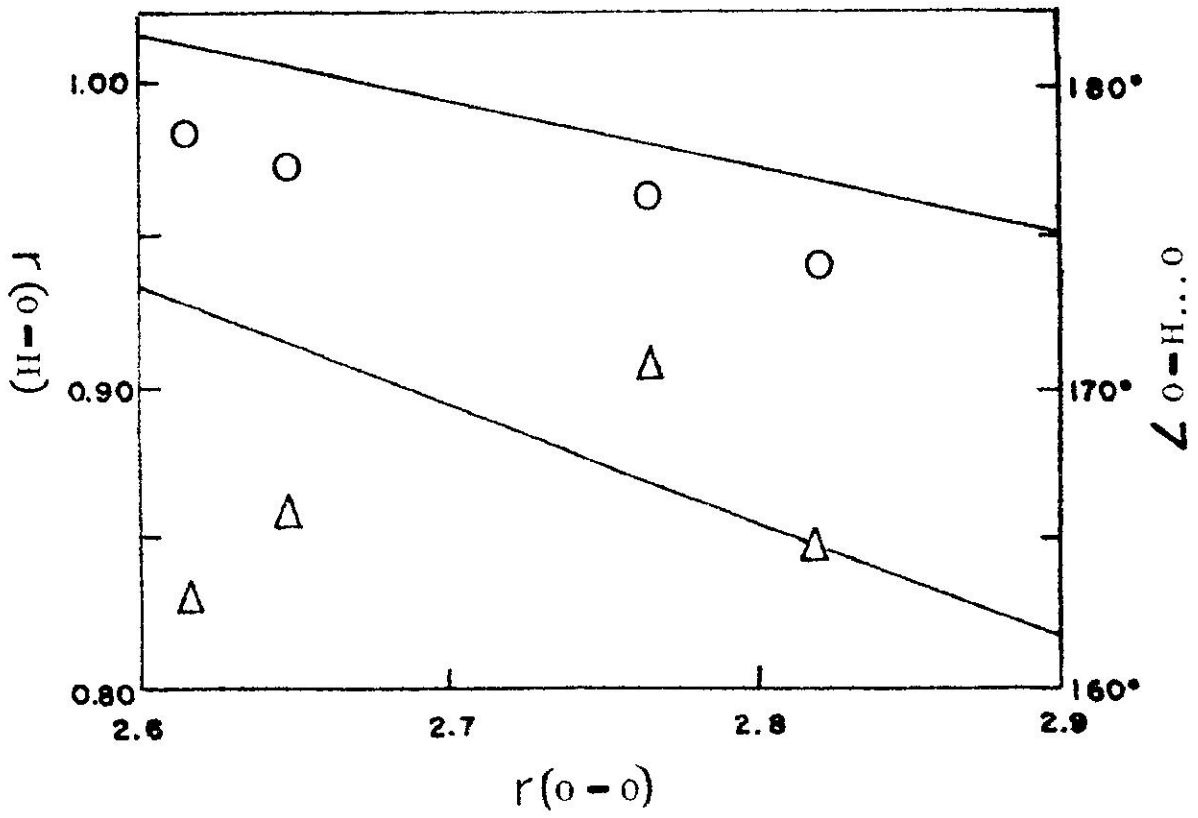

Fig. 9 Plot of O-H distance vs. O-O for Cap Alum, the hydrogen bond distance (circles) and O-H---O angle vs. O-O distance (triangles). The upper line is the empirical function for O-H distance and the lower line is the empirical function for O-H---O angle (Hamilton[21]).

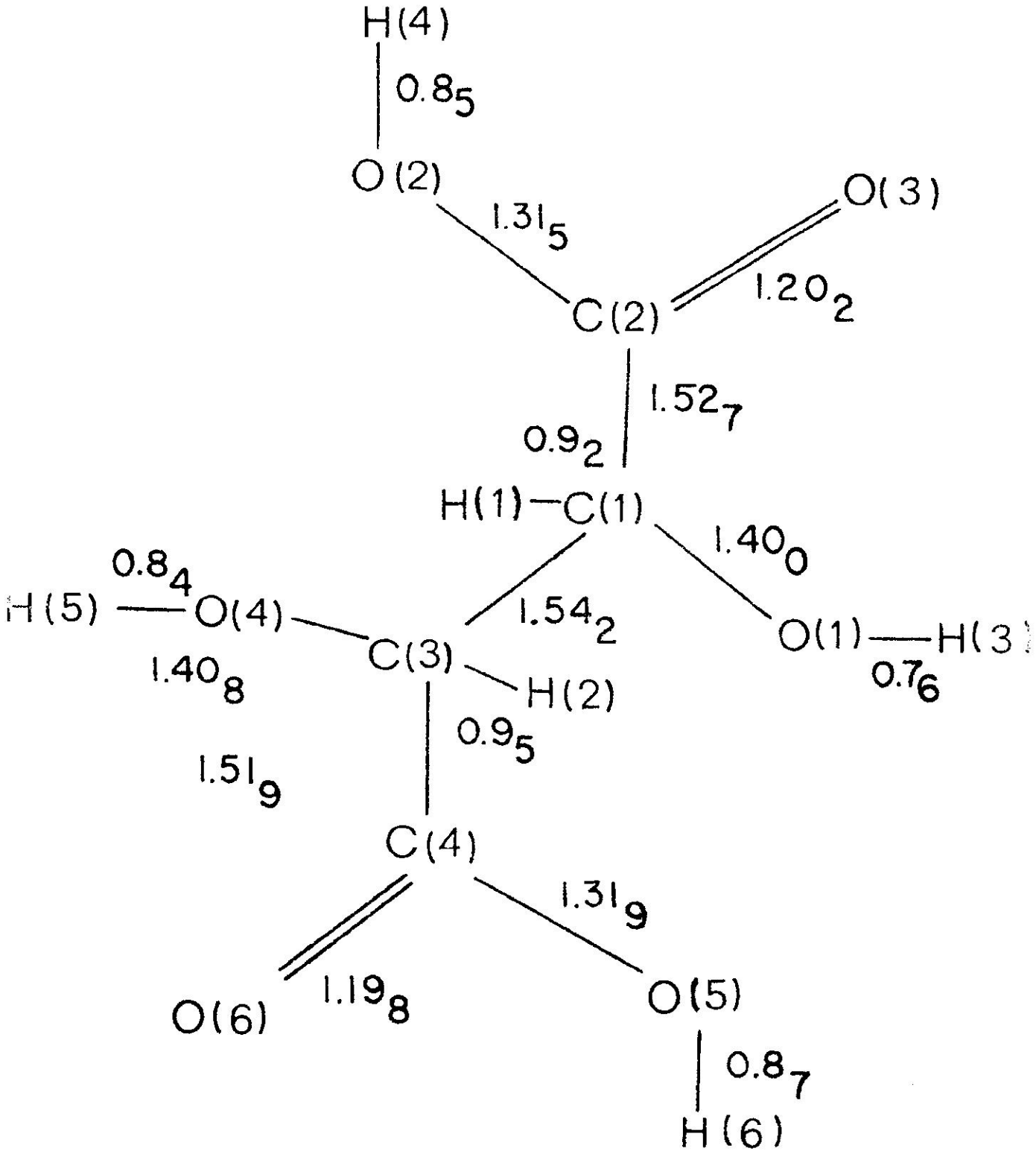

Fig. 10 Bond distances of d-Tartaric Acid from X-ray diffraction.

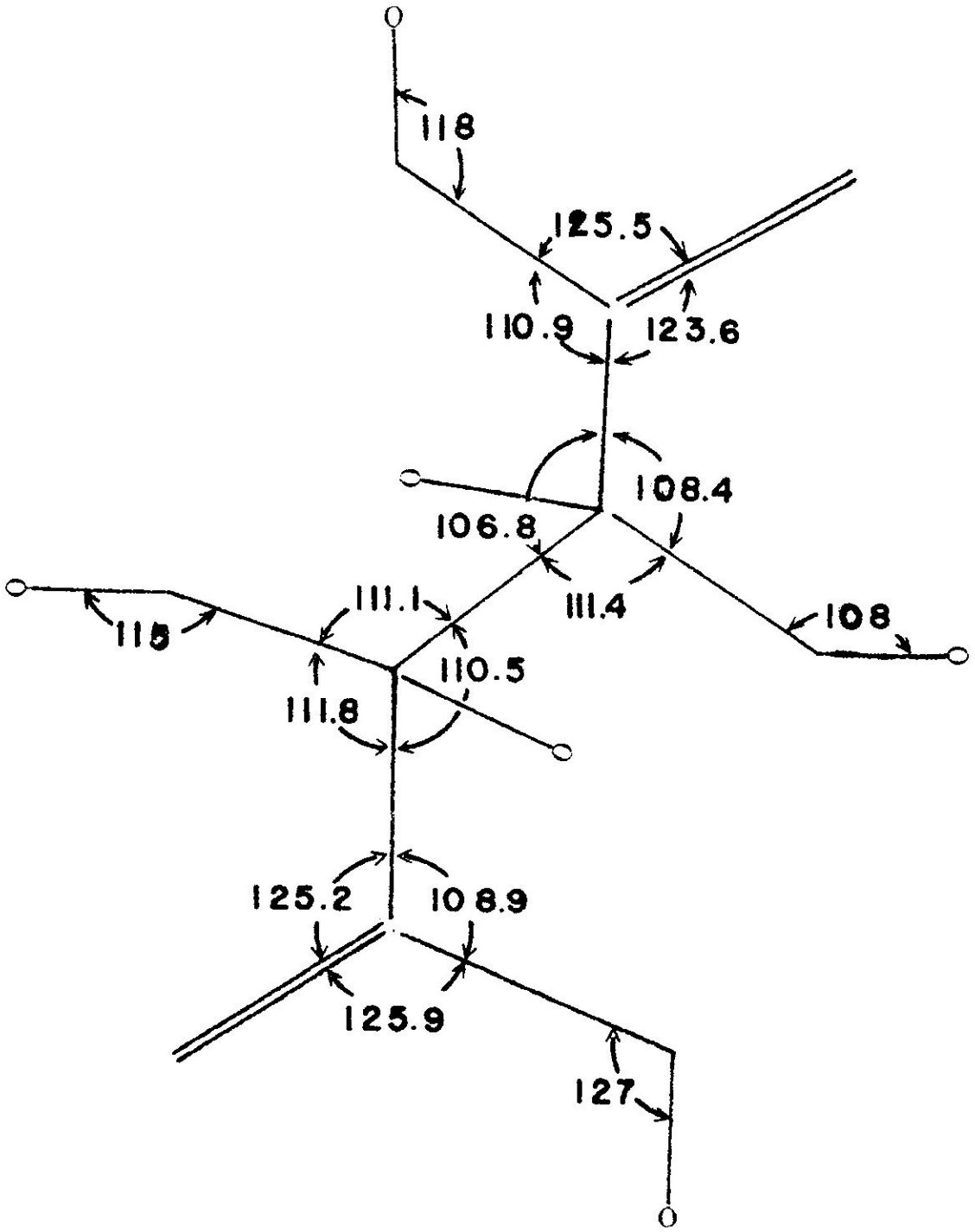

Fig. 11 Bond angles of d-Tartaric Acid from X-ray diffraction

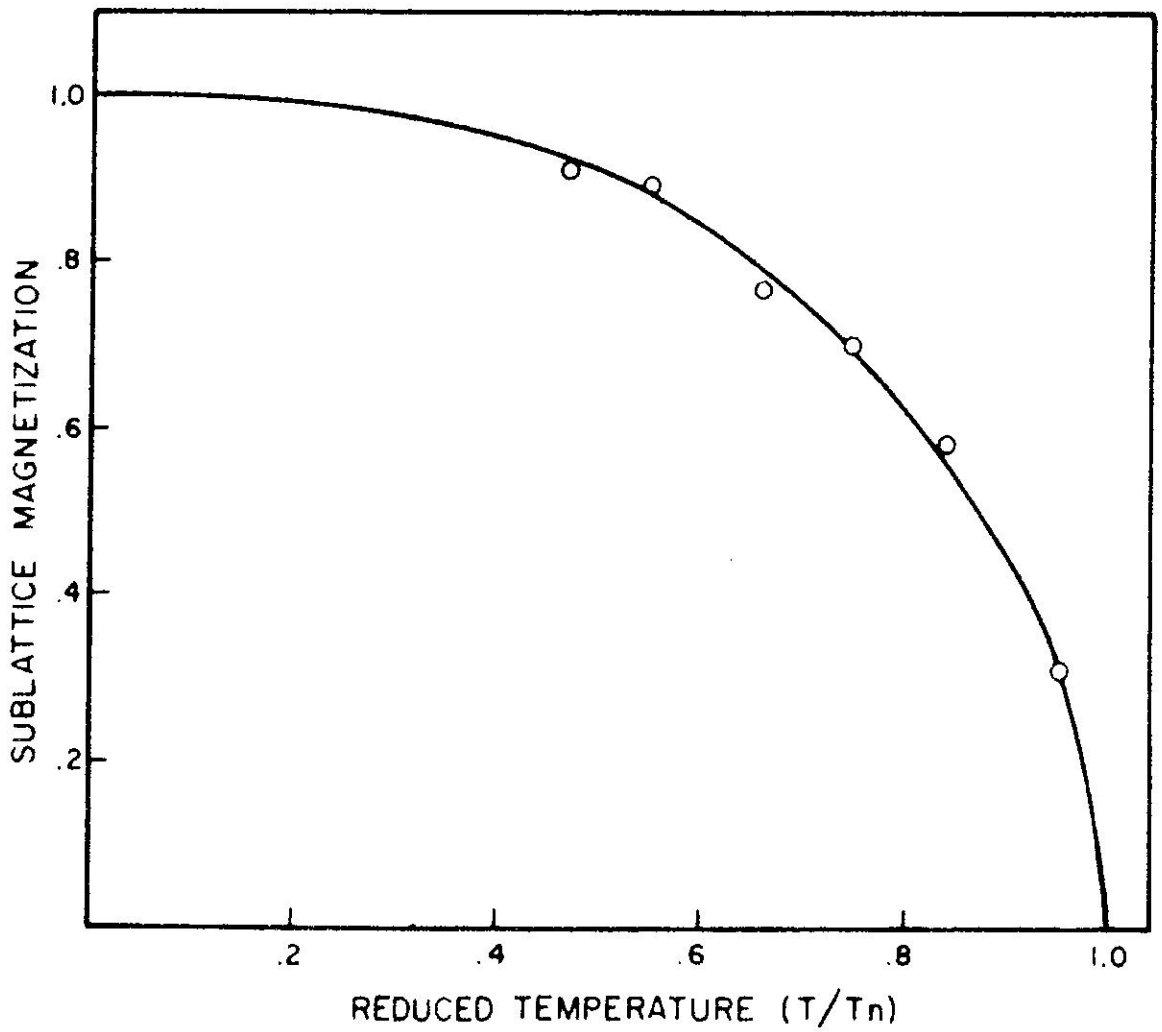

Fig. 12 Sublattice Magnetization vs Reduced Temperature. Circles are the measured points. The line is the Brillouin Function for S = 4/2. (Zeta Pd_3Mn_2)